IEEE Access
Multidisciplinary ⋮ Rapid Review ⋮ Open Access Journal

Received July 7, 2018, accepted August 9, 2018, date of publication August 16, 2018, date of current version September 7, 2018.

Digital Object Identifier 10.1109/ACCESS.2018.2865598

Multiobjective Robust Scheduling for Smart Distribution Grids: Considering Renewable Energy and Demand Response Uncertainty

WENFEI YI, (Student Member, IEEE), YIWEI ZHANG, (Student Member, IEEE), ZHIBIN ZHAO, (Member, IEEE), AND YONGZHANG HUANG, (Member, IEEE)
State Key Laboratory of Alternate Electrical Power System with Renewable Energy Sources, North China Electric Power University, Beijing 102206, China
Corresponding author: Wenfei Yi (yiwenfei2006@163.com)

This work was supported by the National Key Research and Development Program of China under Grant 2016YFB0101900.

ABSTRACT The fluctuating nature of renewable energy is a key factor that limits large-scale integration with the power grid. In this paper, a new method of utilizing multitype demand response (DR) resources to smooth fluctuations in renewable energy on different timescales is proposed. A multiobjective robust scheduling model considering renewable energy and DR uncertainties is established using this method. First, the robust optimization theory is introduced, and uncertainties in renewable energy and multitype DR resources are described in the form of robust intervals on multiple timescales. Then, the multiobjective scheduling model is constructed with the objective of obtaining the lowest operating cost and the highest renewable energy utilization rate, while considering renewable energy integration constraints, DR output constraints, and system power balance constraints. Finally, according to the model characteristics, the uncertainty problem is transformed into a deterministic problem by using a robust counterpart transformation, and a nondominated set genetic algorithm-II is used to solve the deterministic problem. A case study is presented to verify the effectiveness of the proposed scheduling model and solution method. The calculation results show that multitype DR resources can effectively smooth fluctuations in renewable energy, and the proposed robust scheduling method can increase the robustness of the scheduling plan.

INDEX TERMS Renewable energy generation, fluctuating nature of renewable energy, multitype demand response, uncertainty, multiobjective robust scheduling.

I. INTRODUCTION

The development of renewable energy generation (REG) is an important goal for future energy systems [1]. In recent years, driven by policies such as energy conservation and emission reduction, REG has gradually been integrated on a large scale. However, unlike conventional types of generation, such as thermal power generation and natural gas power generation, REG is usually highly intermittent and fluctuant. Therefore, the large-scale integration of REG faces a substantial challenge for the power grid.

To effectively smooth fluctuations and improve the integration of REG, the usual practice is to increase the supply-side investment, i.e., by configuring deeper peaking units [3], transferring electric energy across regions [4] and installing energy storage devices [5], [6]. However, the use of supply-side resources to solve the large-scale integration of renewable energy often faces many difficulties in practice, such as high investment costs and poor equipment flexibility [7]. In a smart grid, due to the application of modern information and communication technologies, demand-side resources can be used as a type of virtual power generation resource and can participate in power system operation and management. Therefore, demand response (DR) is introduced to smooth the fluctuations in renewable energy, providing a new and important way to resolve the large-scale integration and efficient operation of REG [8], [9].

Several studies focus on using DR resources to smooth fluctuations in renewable energy and promote the integration of renewable energy. Reference [10] proposes that DR resources can be used as a virtual power generation resource to include in the joint scheduling of power systems, which can effectively reduce system operating costs. In [11], an energy management system (EMS) is proposed to optimize the operation of REG. Through the integration of demand-side management (DSM) and an active management scheme (AMS), an EMS can make good use of renewable energy and reduce customer energy consumption costs while increasing the economic and environmental benefits. Reference [12] uses a probability distribution function to model the prediction errors of wind speed and solar radiation and establishes a two-stage stochastic optimization scheduling model with the objective of minimizing expected operating costs. In [13], own-price and cross-price elasticity models are proposed to integrate the short-term DR into the unit commitment optimization model for DR and renewable energy joint scheduling. Reference [14] establishes a two-stage stochastic optimal scheduling model that considers the wind power and load forecasting errors, as well as the unit random safety constraints. In [15], a DR model based on game theory is established and applied to a multiobjective dynamic economic dispatch. Reference [16], using the idea of rolling scheduling, establishes a joint decision model for renewable energy and DR based on day-ahead and real-time timescales, in which the day-ahead optimization results are applied to real-time scheduling decisions. Reference [17] considers uncertainties in renewable energy, price, and load forecasting; the study establishes a stochastic optimal scheduling model for power grids that uses renewable energy as the main power source, while an external power supply and DR resources are used as backups.

The above research studies the participation of DR resources in a smart grid. However, two problems need to be further explored regarding the use of DR resources to smooth fluctuations in renewable energy on multiple timescales. First, the existing research mostly focuses on the joint scheduling of DR resources, renewable energy, and conventional power generation resources from multiple timescales. However, the utilization of the complementarity in the responses of different types of DR resources to more effectively smooth fluctuations in renewable energy on different timescales is rarely studied. Second, the existing research often uses random optimization, fuzzy optimization and other methods to address the uncertainty of DR or even ignore it; however, for random optimization, due to information privacy or other reasons, an accurate probability distribution of the available capacities of DR resources at each timescale is often difficult for decision makers to obtain, which complicates the effective application of random optimization to the above problems [18], [19]. Additionally, in the fuzzy optimization method, the determination of the membership function is highly dependent on the sample data and the experience of the decision maker; therefore, the optimality of the decision is not guaranteed in many cases [20].

Based on the abovementioned problems, this paper proposes a multiobjective robust scheduling method for multitype DR resources and renewable energy on multiple timescales. Different from stochastic optimization and fuzzy optimization, the robust optimization method describes the range of variation in uncertain variables through an interval that avoids the need for a probability distribution of variables [21]. First, this paper establishes a robust interval model for the uncertainties in the output of renewable energy power generation and DR. Then, with the two objectives of lowest system operating cost and highest renewable energy utilization, a multiobjective optimal scheduling model is established that considers the constraints of REG fluctuations, DR resource availability, and system power balance. The multiobjective model focuses on the use of DR resources on different timescales. When the model is solved, the counterpart transformation is introduced to convert the uncertain problem into a deterministic problem, and then a nondominated set ranking multiobjective genetic algorithm with the elite strategy (NSGA-II) is used to solve the problem. Finally, the case study for a distribution grid is presented to verify the validity of the proposed model and method.

II. UNCERTAINTY DESCRIPTION OF RENEWABLE ENERGY AND DEMAND RESPONSE

In a smart distribution grid, uncertainties usually come with renewable energy and DR. In the robust optimization method, the uncertainty is usually described in the form of robust intervals as a set of parameters that contains infinite scenarios. Therefore, in this section, we describe the uncertainties of renewable energy and DR output as the robust intervals.

A. UNCERTAINTY DESCRIPTION OF RENEWABLE ENERGY GENERATION

Due to the influence of the natural environment, REG has a high degree of random fluctuations. Minute-level to hour-level fluctuations often affect generation reserves and generation scheduling; while second-level to minute-level fluctuations affect the frequency regulation of the power system [22]. Different countries have different restrictions regarding the fluctuation of renewable energy for grid integration. For example, China has set maximum limits on the rate of change in active power during 1 min and 10 min for renewable energy integration [23].

The amplitude-frequency characteristics of REG exhibit large differences for different timescales. The fluctuations on short timescales possess a high frequency and large amplitude, while the fluctuations on long timescales have a low frequency and small amplitude. Therefore, to achieve an exact match with relevant DR resources, classifying the uncertainty characteristics of REG on different timescales is necessary.

To achieve the abovementioned goals, the output curve of the day-ahead prediction of renewable energy is divided into a smooth part, a long-timescale fluctuation part and a short-timescale fluctuation part according to the wavelet decompositions the long timescale (10 min) and short timescale (1 min) [24]. The relevant mathematical equations are as follows:

$$\overline{P}_{re}(t) = \overline{P}_{smo}(t) + \overline{P}_{short}(t) + \overline{P}_{long}(t) \tag{1}$$

where $\overline{P}_{re}(t)$ is the day-ahead predicted output of the renewable energy, $\overline{P}_{smo}(t)$ is the smooth part, $\overline{P}_{long}(t)$ is the long-timescale fluctuation part, and $\overline{P}_{short}(t)$ is the short-timescale fluctuation part. Since a deviation between the actual output and the day-ahead predicted output of the renewable energy exists, the uncertainties will need to be considered when making a scheduling plan. Based on (1), the smooth part and the wave parts mentioned above are given in different timescales by (2), (3), and (4):

$$P_{smo}(t) = \overline{P}_{smo}(t) + \xi_{smo}\hat{P}_{smo}(t) \tag{2}$$

$$P_{long}(t) = \overline{P}_{long}(t) + \xi_{long}\hat{P}_{long}(t) \tag{3}$$

$$P_{short}(t) = \overline{P}_{short}(t) + \xi_{short}\hat{P}_{short}(t) \tag{4}$$

where $P_{smo}(t)$, $P_{long}(t)$, and $P_{short}(t)$ represent the smooth part, the long-timescale part and the short-timescale part of the actual output, respectively; $\hat{P}_{smo}(t)$, $\hat{P}_{long}(t)$, and $\hat{P}_{short}(t)$ represent the upper limits of deviation for the smooth part, the long-timescale part and the short-timescale part between the actual output and the day-ahead predicted output, respectively; and ξ_{smo}, ξ_{long}, and ξ_{short} are the uncertainty parameters that represent the uncertainty level of the deviation between the actual output and the predicted output. The uncertainty parameters can be given by (5):

$$\xi_{smo}, \xi_{long}, \xi_{short} \in [-1, 1] \tag{5}$$

The uncertainty parameters given above are used to describe the output of the renewable energy in the following scheduling models.

B. UNCERTAINTY DESCRIPTION OF THE DR

In a smart grid, there are various types of DR projects. Among them, the incentive-based DR(IBDR) presents a shorter early notification time and response time, which yield greater potential for smoothing the fluctuations in renewable energy and promoting the large-scale grid integration of renewable energy [25]. Therefore, this paper mainly focuses on an optimal scheduling model based on the IBDR.

In a smart distribution grid, when the fluctuations in renewable energy output are increased, the DR can immediately regulate the load demand to smooth the fluctuations after receiving relevant notifications. According to the response time and response direction of the incentive DR, this paper divides the overall IBDR into four types: direct controlled interruptible load (DI), direct controlled shifting load (DS), nondirect controlled interruptible load (NDI), nondirect controlled shifting load (NDS). The response time represents the timescale of each type of DR when it participates in the system scheduling. The response direction represents the increase or reduction of the load on the demand side. The operating statuses of the IBDRs are shown in Table 1.

In Table 1, the "ascending" indicates that the IBDR increases the power demand by means of shifting load, and the "descending" indicates that the IBDR reduces the power demand by cutting off load.

For IBDR projects, based on the day-ahead scheduling plan, grid companies generally interact with DR resource providers (load aggregators or customers) in the form of contracts to determine the response capacity.

TABLE 1. Multitype demand response characteristics.

Type	Response Time	Response Direction
DI	1 min level	descending
DS	1 min level	descending / ascending
NDI	10 min level	descending
NDS	10 min level	descending / ascending

For DI and DS, the actual response output is equal to the contracted capacity since these loads are directly controlled by the grid companies:

$$P^j_{di}(t) = \overline{P}^j_{di}(t) \tag{6}$$

$$P^j_{ds}(t) = \overline{P}^j_{ds}(t) \tag{7}$$

where $P^j_{di}(t)$ and $\overline{P}^j_{di}(t)$ are the actual output and the contracted response capacity of the DI, respectively, that customer j offered in the period of t, while $P^j_{ds}(t)$ and $\overline{P}^j_{ds}(t)$ are the actual output and the contracted response capacity of the DS, respectively, that customer j offered in the period of t.

However, for NDI and NDS, considering the uncertainties of the user behavior and willingness to respond, the actual response will present a certain degree of uncertainty, so the actual response output is derived with the contracted capacity. In the robust optimization method, the interval forms can also be used to describe this uncertainty:

$$P^j_{ndi}(t) = \overline{P}^j_{ndi}(t) + \xi^j_{ndi}\hat{P}^j_{ndi}(t) \tag{8}$$

$$P^j_{nds}(t) = \overline{P}^j_{nds}(t) + \xi^j_{nds}\hat{P}^j_{nds}(t) \tag{9}$$

where $P^j_{ndi}(t)$ and $\overline{P}^j_{ndi}(t)$ are the actual output and the contracted response capacity of the NDI, respectively, that customer j offered in the period of t; $P^j_{nds}(t)$ and $\overline{P}^j_{ndi}(t)$ are the actual output and the contracted response capacity of the NDS, respectively, that customer j offered in the period of t; $\hat{P}^j_{ndi}(t)$ and $\hat{P}^j_{nds}(t)$ are the upper limits of the deviation between the actual output and the contracted response capacity, which can be obtained from the history operation data; ξ^j_{ndi} and ξ^j_{nds} are uncertainty parameters representing the uncertainty level of the deviation between the actual output and the contracted response capacity:

$$\xi^j_{ndi}, \xi^j_{nds} \in [-1, 1] \tag{10}$$

The uncertainty parameters given above are used to describe the output of the DR in the following scheduling models.

III. MULTIOBJECTIVE ROBUST SCHEDULING MODEL

A. PROBLEM DESCRIPTION

In day-ahead optimization scheduling, if the response capacity of the DR is increased, then the effect of smoothing the fluctuations in renewable energy is usually better, and the system can increase the utilization rate of renewable energy; however, the incentive subsidies (costs) paid to the providers are also higher. If the response capacity of the DR is decreased, the cost of the DR is reduced, and the integration rate of the renewable energy is also decreased. Therefore, the proposed multiobjective robust scheduling model is designed to achieve a balance of economic system operation and environmental benefits by scheduling the different types of DR resources, renewable energy and external power supply properly, as well as on the basis of the constraints of renewable energy integration and the safe operation of the system. The objective functions of the model include two goals, which are minimizing the operation cost of the distribution grid and maximizing the utilization rate of renewable energy.

Based on the abovementioned considerations, the multiobjective robust scheduling model framework is shown below in Figure 1.

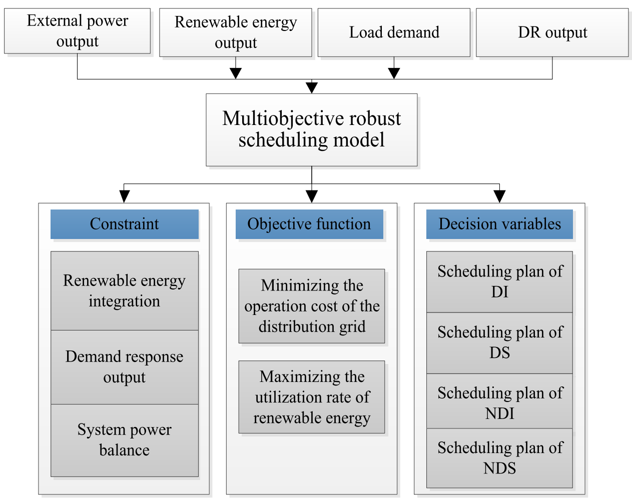

FIGURE 1. **Framework of the multiobjective robust scheduling model.**

B. OBJECTIVE FUNCTION

1) OPERATING COST OF THE DISTRIBUTION GRID

In the distribution grid with the DR and renewable energy, the operational cost includes the DR costs paid to the providers and the cost of purchasing electricity from the external power grid. The operating cost is calculated by (11) as follows:

$$f1 = \sum_{j=1}^{N_{dr}} \sum_{t=1}^{T} \left[\overline{P}_{di}^{j}(t) \cdot \rho_{di}(t) + \overline{P}_{ds}^{j}(t) \cdot \rho_{ds}(t) \right] + \sum_{j=1}^{N_{dr}} \sum_{t=1}^{T} \left[\overline{P}_{ndi}^{j}(t) \cdot \rho_{ndi}(t) + \overline{P}_{nds}^{j}(t) \cdot \rho_{nds}(t) \right] + \sum_{t=1}^{T} P_{ext}(t) \cdot \rho_{ext}(t) \quad (11)$$

where N_{dr} is the number of providers that offer DR resources; T is the total number of scheduling periods; $\rho_{di}(t)$, $\rho_{ds}(t)$, $\rho_{ndi}(t)$, and $\rho_{nds}(t)$ represent the prices of the DI, DS, NDI, and NDS, respectively, in the period of t; $P_{ext}(t)$ is the power purchased from the external power grid in the period of t; and $\rho_{ext}(t)$ is the price of the power purchased from the external power grid in the period of t.

2) UTILIZATION RATE OF RENEWABLE ENERGY

After using the multitype DR resources to smooth the fluctuations in renewable energy, the grid-connected power from renewable energy can be calculated by (12):

$$P_{out}(t) = \overline{P}_{re}(t) + \sum_{j=1}^{N_{dr}} \left[\overline{P}_{di}^{j}(t) + \overline{P}_{ds}^{j}(t) \right] + \sum_{j=1}^{N_{dr}} \left[\overline{P}_{ndi}^{j}(t) + \overline{P}_{nds}^{j}(t) \right] + P_{desert}(t) \quad (12)$$

where $P_{out}(t)$ is the grid-connected power from renewable energy, and $P_{desert}(t)$ is the abandoned power from REG.

Based on (12), the utilization rate of renewable energy in the distribution grid can be expressed as the ratio of the grid-connected power to the total power from renewable energy and is calculated by (13):

$$f_2 = \sum_{t=1}^{T} P_{out}(t) / \sum_{t=1}^{T} \overline{P}_{re}(t) \quad (13)$$

C. CONSTRAINTS

1) RENEWABLE ENERGY INTEGRATION CONSTRAINTS

The fluctuations in renewable energy will affect the power quality and reliability of the distribution grid, and excessive fluctuations may even affect grid stability; therefore, the fluctuations in renewable energy are limited regarding integration with the power grid. According to the renewable energy integration regulations in [23], when renewable energy is integrated into the power gird, the fluctuation rate of active power should not exceed 10% in 1 min and 33% in 10 min.

To accurately describe the above constrains, the short-term scale (1 min) is taken as an example to illustrate the integration constraints of renewable energy. Assuming that the sampling period of renewable energy is Δt, then according to (12), the change in the grid-connected power from renewable energy between t_0 and $t_0 + \Delta t$is calculated by (14) as follows:

$$\Delta P_{short}(t_0) = P_{out}(t_0 + \Delta t) - P_{out}(t_0) \quad (14)$$

where $\Delta P_{short}(t_0)$ is the change in the grid-connected power from the renewable energy between t_0 and $t_0 + \Delta t$. Using (14), each change in the grid-connected power from renewable energy from t_0 to $(t_0 + 1)$ for the short timescale (1 min) is calculated, and then, the maximum power fluctuation $\Delta P_{short}^{\max}(t_0)$is selected. In day-ahead scheduling, the maximum power fluctuation $\Delta P_{short}^{\max}(t)$ in each $(t + 1) - t$ period can be selected. Therefore, for each period of t, the integration constraint of renewable energy for the short timescale is determined by (15):

$$\Delta P_{short}^{\max}(t) / P_{out}(t) \leq 10\% \quad (15)$$

Similarly, for the long timescale (10 min), the maximum power fluctuation during each $(t + 10) - t$ period can be calculated, and for each period of t, the integration constraint of renewable energy for the long timescale is depicted in (16):

$$\Delta P_{long}^{\max}(t)/P_{out}(t) \leq 33\% \tag{16}$$

2) DR OUTPUT CONSTRAINTS

In the scheduling process, due to the characteristics of the DR, there are specific constraints on the response capacity and response speed. Taking the DI as an example, the constraints of the DR output are given in (17), (18) and (19).

The constraint of the maximum response capacity is described in (17):

$$0 \leq P_{di}^{j}(t) \leq M_{di}^{j}(t) \tag{17}$$

where $M_{di}^{j}(t)$ is the maximum capacity for the DI response of customer j in period t.

The constraints of the response speed are described in (18) and (19):

$$P_{di}^{j}(t+1) - P_{di}^{j}(t) \leq U_{di}^{j}(t) \tag{18}$$

$$P_{di}^{j}(t+1) - P_{di}^{j}(t) \leq D_{di}^{j}(t) \tag{19}$$

where $U_{di}^{j}(t)$ is the maximum ascending speed of the DI response of user j in period t, and $D_{di}^{j}(t)$ is the maximum descending speed of the DI response of user j in period t.

3) POWER BALANCE CONSTRAINS

For the operation of the distribution grid, the system operator can comprehensively use the renewable energy output, external gird output and DR to satisfy the end-customer load demand. Therefore, the constraint of the power balance can be described as (20):

$$\begin{aligned} P_{load}(t) = P_{ext}(t) + P_{re}(t) + \sum_{j=1}^{N_{dr}} \left[\overline{P}_{di}^{j}(t) + \overline{P}_{ds}^{j}(t)\right] \\ + \sum_{j=1}^{N_{dr}} \left[\overline{P}_{ndi}^{j}(t) + \overline{P}_{nds}^{j}(t)\right] + P_{desert}(t) \end{aligned} \tag{20}$$

where $P_{load}(t)$ is the active power of the load demand in period t.

The constrains of the other types of DR resources are similar and are not depicted.

IV. MULTIOBJECTIVE ROBUST OPTIMIZATION SOLVING ALGORITHM

The established scheduling model is a typical multiobjective robust optimization problem. As the uncertainty is described in the form of a robust interval, the problem cannot be solved directly. Therefore, performing a robust counterpart transformation of the uncertainties in the model is necessary. First, the robust counterpart transformation is used to transform the uncertain multiobjective problem into a deterministic multiobjective problem. Then, the NSGA-II is implemented to solve the deterministic multiobjective problem.

A. ROBUST COUNTERPART TRANSFORMATION

1) PROCESSING OF THE GENERAL MODEL

The general model of robust optimization is described by (21):

$$\begin{cases} \min\ f_i(x,\xi) \\ s.t.\ g_i(x,\xi) \leq 0, \quad \forall \xi \in U, (i = 1, \ldots, m), x \in X \end{cases} \tag{21}$$

where f_i is the ith objective function, x is the decision variable, g_i is the i th constraint, ξ is the uncertainty coefficient, and U is the set of uncertainty coefficients.

The basic idea of solving the abovementioned robust optimization problem is to convert uncertain problems into deterministic ones through a counterpart transformation. Therefore, the decision variable is first divided into two parts, the deterministic component and the uncertain component:

$$g_i(x,\xi) = \bar{g}_i(x) + \hat{g}_i(x,\xi) \tag{22}$$

According to the robust optimization theory, the robust optimization model should adapt to all uncertainties in the uncertainty set. Therefore, the constraint should match the maximum uncertainty, and according to (21) and (22), the uncertainty constraint can be further rewritten as (23):

$$\bar{g}_i(x) + \max(\hat{g}_i(x,\xi)) \leq 0 \tag{23}$$

For the proposed optimization model, the distribution grid operating cost function f_1 and renewable energy utilization rate function f_2 are transformed into the general form of robust optimization:

$$f_1^* = f_1, f_2^* = -f_2 \tag{24}$$

We move the uncertainties in the constraints to the left side of the equation. In conjunction with the definition of variable uncertainties, the general robust optimization model is rewritten as (25):

$$\begin{cases} \min\ (f_1^*, f_2^*) \\ \sum_j \bar{a}_{ij} + [\max_{\xi \in U}\{\sum_{j \in J} \xi_j \hat{a}_{ij}\}] \leq b_i \end{cases} \tag{25}$$

where f_1^* is the operation cost of the distribution grid, f_2^* is the negative value of the renewable energy utilization rate, $\bar{a}_{ij}$ is the deterministic component of the decision variable, and $\hat{a}_{ij}$ is the upper limit of the uncertain component.

2) COUNTERPART TRANSFORMATION

From (25), we can see that the rewritten optimization model is a two-stage optimization problem. The model contains a variety of uncertainties and couplings between maximum and minimum values, so the model will be difficult to solve. In this paper, we adopt the dual cone method to carry out the counterpart transformation of the two-stage optimization. The second-order dual cone method is briefly described below.

The set U_j of the uncertainty coefficients ξ_{ij} is depicted in (26):

$$U_j = \left\{ \xi \left| \sum_{j \in J} |\xi_j| \le \mu\Gamma \right., \xi_j \in [-1, 1] \right\}$$
$$\mu \in [-1, 1], \Gamma \in [0, L] \tag{26}$$

where Γ is the total uncertainty, $\mu$is the adjustable robust coefficient, and L is the upper limit of the robust interval; μ can be adjusted to control the robustness of each variable in the robust optimization.

Then, two matrices are defined:

$$M_1 = [I_{L\times L}; 0_{1\times L}]$$
$$m_1 = [0_{L\times 1}; \Gamma] \tag{27}$$

The convex cone is given as follows:

$$K_1 = \{[\tau_{L\times 1}; t] \in R^{L+1} \,|\, \|\tau\|_1 \le t\} \tag{28}$$

$\max\limits_{\xi \in U}\{\sum\limits_{j\in J} \xi_{ij}\hat{a}_{ij}\}$ can be described as follows:

$$\max_{\xi}\{\sum_{j\in J} \xi_{ij}\hat{a}_{ij} : M_1\xi + m_1 \in K_1\} \tag{29}$$

(29) describes the ∞ norm cone, and the dual of the ∞ norm cone is the 1 norm cone:

$$\sup\{z^T x \,|\, \|x\|_\infty \le 1\} = \sum_{i=1}^{n} |z_i| = \|z\|_1 \tag{30}$$

$$K_\infty^* = K_1 = \{[\tau_{L\times 1}; t] \in R^{L+1} \,|\, \|\tau\|_\infty \le t\} \tag{31}$$

In summary, the constraints can be converted to (32):

$$\max_{\xi \in U}\{\sum_{j\in J} \xi_{ij}\hat{a}_{ij}\}^* = \Gamma \max(\hat{a}_{ij}) \tag{32}$$

Therefore, the constraints in the proposed optimization model can be transformed into (33)-(41):

$$\overline{P}^j_{ndi}(t) \ge 0 \tag{33}$$
$$\overline{P}^j_{ndi}(t) + \Gamma^j_{ndi}(t) \cdot \max(\hat{P}^j_{ndi}) \le M^j_{ndi}(t) \tag{34}$$
$$[\Delta\overline{P}_{short}(t) + \Gamma_{short}(t) \cdot \max(\hat{P}_{short}(t))]/\overline{P}_{out}(t) \le 10\% \tag{35}$$
$$[\Delta\overline{P}_{long}(t) + \Gamma_{long}(t) \cdot \max(\hat{P}_{long}(t))]/\overline{P}_{out}(t) \le 33\% \tag{36}$$
$$\overline{P}^j_{ndi}(t+1) - \overline{P}^j_{ndi}(t) + \Gamma^j_{ndi}(t+1) \cdot \max[\hat{P}^j_{ndi}(t+1)] + \Gamma^j_{ndi}(t) \cdot \max[\hat{P}^j_{ndi}(t)] \le U^j_{ndi}(t) \tag{37}$$
$$\overline{P}^j_{ndi}(t) - \overline{P}^j_{ndi}(t+1) + \Gamma^j_{ndi}(t) \cdot \max[\hat{P}^j_{ndi}(t)] + \Gamma^j_{ndi}(t+1) \cdot \max[\hat{P}^j_{ndi}(t+1)] \le D^j_{ndi}(t) \tag{38}$$
$$\overline{P}^j_{nds}(t+1) - \overline{P}^j_{nds}(t) + \Gamma^j_{nds}(t+1) \cdot \max[\hat{P}^j_{nds}(t+1)] + \Gamma^j_{nds}(t) \cdot \max[\hat{P}^j_{nds}(t)] \le U^j_{nds}(t) \tag{39}$$
$$\overline{P}^j_{nds}(t) - \overline{P}^j_{nds}(t+1) + \Gamma^j_{nds}(t) \cdot \max[\hat{P}^j_{nds}(t)] + \Gamma^j_{nds}(t+1) \cdot \max[\hat{P}^j_{nds}(t+1)] \le D^j_{nds}(t) \tag{40}$$
$$\Gamma = (\Gamma_{ndi}, \Gamma_{nds}, \Gamma_{short}, \Gamma_{long}) \tag{41}$$

where $\Gamma_{ndi}, \Gamma_{nds}$ are the total uncertainties in the DR output, and $\Gamma_{short}, \Gamma_{long}$ are the total uncertainties in REG. The different optimal results under different uncertainties can be obtained by modifying the adjustable robust coefficientμ. The model can also present the influence of any uncertainty on the optimization result.

B. NONDOMINATED SET GENETIC ALGORITHM (NSGA-II)

The objective function in the scheduling model includes the minimum operating cost of the distribution grid and the maximum utilization rate of renewable energy. To solve this multiobjective model, this paper adopts the NSGA-II, which is widely used in multiobjective problems. The calculation process is described below:

(1) Initialization. In the scheduling period, the scheduling plan is randomly initialized, and it is denoted as P_0. Then, the convergence indicator and maximum evolution times are given.
(2) Evolutionary operation. The next genus group is generated by adopting selection, crossover and mutation.
(3) Elite strategy. R_0 is formed by combining the new population with the parent population.
(4) Nondominated set sorting and crowding degree sorting. The nondominated set R_0 is sorted, and the crowding degree of each dominating set is calculated.
(5) Convergence criteria. If the convergence criteria are satisfied or the maximum calculation times are reached, then the calculation is finished. Otherwise, steps (2)-(5) are revisited to generate the next-generation population.

V. CASE STUDY

A. AN ACTUAL DISTRIBUTION GRID

The case study of an actual distribution grid is presented in this paper to verify the validity of the proposed model and algorithm.

The parameters of the renewable energy and load demands for the distribution grid are as follows. There are 74 wind-power generating units, each with a unit capacity of 1.5 MW. The maximum forecast output of renewable energy is 104.58 MW, and the minimum forecast output is 25.35 MW. The total load includes industrial, commercial and residential loads, with a daily maximum forecast load of 148.80 MW and a minimum forecast load of 31.5 MW. There are 427 users in the grid who can provide DR, of which 120 users respond to DI, 205 users respond to NDI, 76 users respond to DS and 55 users respond to NDS.

The day-ahead renewable energy forecast output and load forecast are shown below in Figure 2.

The time-of-use electricity price and multitype DR prices are shown below in Table 2.

The response characteristics of multitype DR resources are shown in Table 3.

B. EFFECT OF THE DR TO SMOOTH THE FLUCTUATION OF RENEWABLE ENERGY

To verify the effect of the DR on the smoothing of renewable energy fluctuations, a comparison of the renewable energy

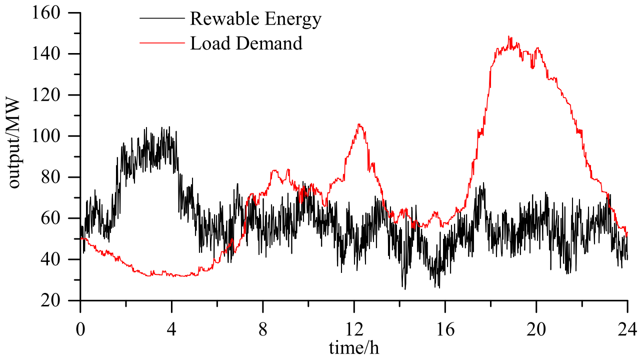

FIGURE 2. Day-ahead forecasting of renewable energy output and load.

TABLE 2. Electricity price and demand response price.

Type	Peak price/¥	Valley price/¥	Flat price/¥
External Electricity	0.8	0.37	0.55
DI	1.8	0.37	0.55
DS	1.6	0.37	0.55
NDI	1.4	0.37	0.55
NDS	1.3	0.37	0.55

TABLE 3. Response capability of demand-side resource.

Type	Max capacity (MW)	Ramp up (MW/min)	Ramp down (MW/min)
DI	12	6	5
DS	14	5	5
NDI	5	2	2
NDS	5	2.5	2.5

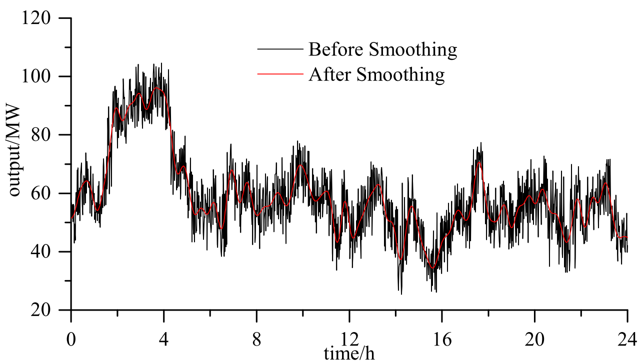

FIGURE 3. The renewable energy output before and after smoothing.

output before and after smoothing is performed. The result is shown below in Figure 3.

Figure 3 reveals that the renewable energy output contains clear fluctuations before smoothing, while the fluctuation magnitude is less after smoothing. Therefore, the DR can effectively smooth the fluctuations in renewable energy.

To further illustrate the smoothing effect of the DR on the fluctuations in renewable energy, we introduce the smoothness criterion proposed in [27]. Taking the smooth part of the renewable energy output as a benchmark, the smoothness of renewable energy before and after smoothing is calculated, with ±10% as the limit. The calculation results are shown in Figure 4.

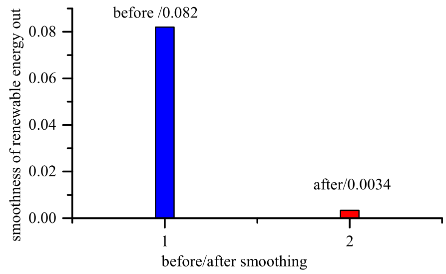

FIGURE 4. Smoothness of renewable energy output before and after smoothing.

By comparing the smoothness values of the output of renewable energy sources before and after smoothing, the fluctuation magnitude of renewable energy is effectively suppressed after adopting multiple types of DRs.

C. INFLUENCE OF ROBUSTNESS ON OPTIMIZATION OBJECTIVE

To verify the influence of different robustness levels on the optimization objectives, 0, 0.5 and 1 are utilized as the adjustable robust coefficient, and the Pareto fronts for different robustness values are calculated. The results are shown in Figures 5 – 7.

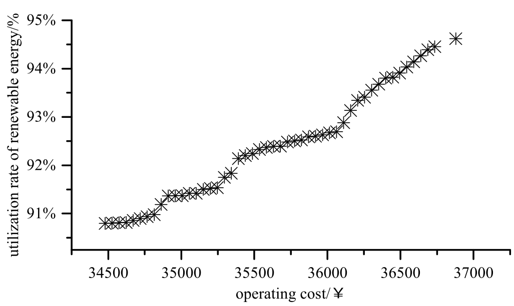

FIGURE 5. Pareto front for $\mu = 0$.

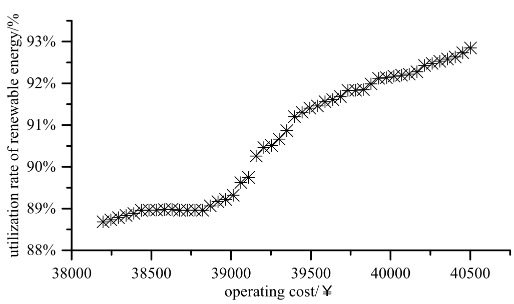

FIGURE 6. Pareto front for $\mu = 0.5$.

Figure 5 and Figure 6 show that compared with deterministic optimization, the operating cost of the grid is significantly increased when the uncertainty in renewable energy and the

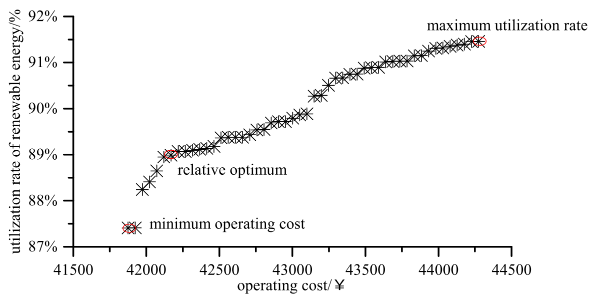

FIGURE 7. Pareto front for $\mu = 1$.

DR is considered. To ensure that renewable energy is effectively integrated into the grid, robust scheduling is required to invoke more DR resources in the extreme scenarios of renewable energy output and DR output, which increases the operating costs of the system.

A comparison of Figures 5 – 7 shows that as the robustness increases, the operating cost of the grid demonstrates a clear upward trend, and the utilization rate of renewable energy gradually declines. Therefore, as the system robustness increases, the uncertainty of the renewable energy output and DR output increases. According to the robust optimization objective, the system needs to maintain operability for all scenarios within the uncertain set; as such, the DR output must be increased, clearly increasing operating costs. At the same time, as the fluctuations in renewable energy increase, the probability of abandoning renewable energy increases; thus, the utilization rate of renewable energy exhibits a downward trend.

D. SCHEDULING PLANS FOR THE DR WITH DIFFERENT OPERATION OBJECTIVES

Taking $\mu = 1$ as the adjustable robust coefficient to illustrate the scheduling plans for different operation objectives, the multiobjective Pareto front is shown in Figure 7. The TOPSIS method proposed in [28] is used to obtain the relative optimal solution. The weights of the operation cost and renewable energy utilization rate are $W = [0.2, 0.8]$. The corresponding points of the maximum utilization rate of renewable energy solution, the minimum operating cost solution, and the relatively optimal solution are shown in red circles in Figure 7. The objective values are as given below in Table 4.

TABLE 4. Objective values for different schemes.

Operation objective	Utilization rate of renewable energy	Operating cost /￥
maximum utilization rate of renewable energy	91.5%	44256
minimum operating cost	87.4%	41904
relative optimum	89.0%	42235

Taking time (3:00-4:00) when the renewable energy output at peak as an example, Figures 8 to 10 show the DR plan outputs under different scheduling objectives. The positive value

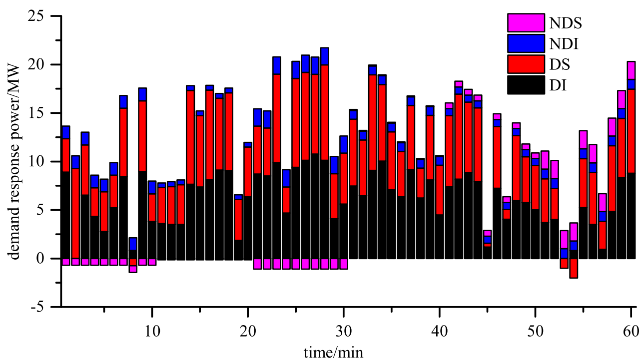

FIGURE 8. DR power under maximum renewable energy utilization.

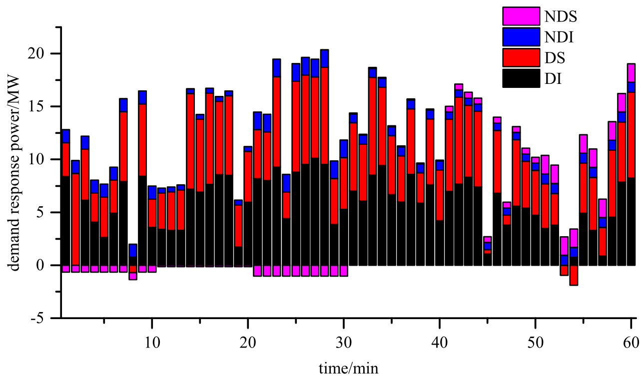

FIGURE 9. DR power under minimum operating cost.

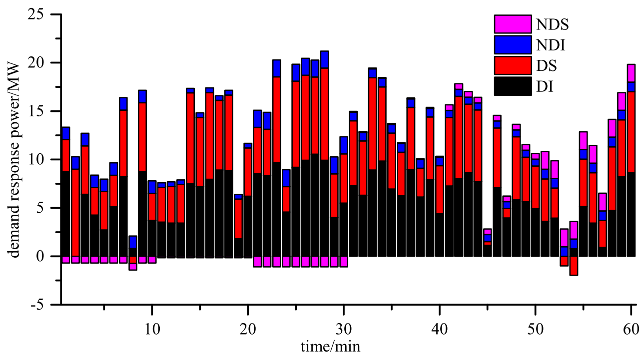

FIGURE 10. DR power under relative optimum.

indicates a load reduction, while the negative value indicates a load increase. For the DI and NDI, the DR power assumes a positive value for load reduction. Since the response power cannot increase the load, there is no case in which its value is negative. For the DS and NDS, the DR power is positive for a load reduction, and the DR power is negative for a load increase.

A comparison of Figure 8 with Figure 10 shows that, due to the contrasting goals of maximum utilization rate of renewable energy and minimum operating cost, as the utilization rate of renewable energy increases, the DR output and operating cost increase, whereas the utilization rate of renewable energy decreases with the operating cost of the system. Therefore, the distribution network operators can reasonably formulate scheduling plans based on actual needs to achieve a balance between the maximum utilization rate of renewable energy and minimum operating cost.

VI. CONCLUSION

This paper proposes a new method that uses multitype DR resources to co-smooth fluctuations in renewable energy. Considering the uncertainties of renewable energy output and the DR, a multiobjective robust scheduling model is established. The model is solved using a robust counterpart transformation method and a multiobjective genetic algorithm. The case study of an actual distribution grid is evaluated to verify the validity of the proposed model and algorithm. The results show the following:

Utilizing the response characteristics of multitype DR resources at different timescales can effectively smooth the fluctuations in renewable energy and increase the utilization rate of renewable energy.

The robust optimization model can address the uncertainty problems of both supply and demand sides, which are unsolvable in the traditional deterministic model, and the optimization scheme can satisfy all extreme scenarios.

Given the uncertainty of demand/load increases, to ensure the reliability of the optimization results, the system must balance operating costs with renewable energy utilization.

REFERENCES

[1] R. E. H. Sims, H.-H. Rogner, and K. Gregory, "Carbon emission and mitigation cost comparisons between fossil fuel, nuclear and renewable energy resources for electricity generation," *Energy Policy*, vol. 31, no. 13, pp. 1315–1326, Oct. 2003.

[2] Q. Ai, X. Wang, and X. He, "The impact of large-scale distributed generation on power grid and microgrids," *Renew. Energy*, vol. 62, no. 3, pp. 417–423, Feb. 2014.

[3] H. Lund *et al.*, "4th generation district heating (4GDH): Integrating smart thermal grids into future sustainable energy systems," *Energy*, vol. 68, pp. 1–11, Apr. 2014.

[4] T. J. Hammos *et al.*, "State of the art in ultrahigh-voltage transmission," *Proc. IEEE*, vol. 100, no. 2, pp. 360–390, Feb. 2012.

[5] P. A. Østergaard, "Comparing electricity, heat and biogas storages' impacts on renewable energy integration," *Energy*, vol. 37, no. 1, pp. 255–262, Jan. 2012.

[6] S. Weitemeyer, D. Kleinhans, T. Vogt, and C. Agert, "Integration of renewable energy sources in future power systems: The role of storage," *Renew. Energy*, vol. 75, pp. 14–20, Mar. 2015.

[7] F. Shariatzade, P. Mandal, and A. K. Srivatsava, "Demand response for sustainable energy systems: A review, application and implementation strategy," *Renew. Sustain. Energy Rev.*, vol. 45, pp. 343–350, May 2015.

[8] J. Aghaei and M.-I. Alizadeh, "Demand response in smart electricity grids equipped with renewable energy sources: A review," *Renew. Sustain. Energy Rev.*, vol. 18, pp. 64–72, Feb. 2013.

[9] B. Zeng, J. Zhang, X. Yang, J. Wang, J. Dong, and Y. Zhang, "Integrated planning for transition to low-carbon distribution system with renewable energy generation and demand response," *IEEE Trans. Power Syst.*, vol. 29, no. 3, pp. 1153–1165, May 2014.

[10] H.-G. Kwag and J.-O. Kim, "Optimal combined scheduling of generation and demand response with demand resource constraints," *Appl. Energy*, vol. 96, no. 1, pp. 161–170, Aug. 2012.

[11] C. Cecati, C. Citro, and P. Siano, "Combined operations of renewable energy systems and responsive demand in a smart grid," *IEEE Trans. Sustain. Energy*, vol. 2, no. 4, pp. 468–476, Oct. 2011.

[12] M. Mazidi, A. Zakariazadeh, S. Jadid, and P. Siano, "Integrated scheduling of renewable generation and demand response programs in a microgrid," *Energy Convers. Manage.*, vol. 86, pp. 1118–1127, Oct. 2014.

[13] C. De Jonghe, B. F. Hobbs, and R. Belmans, "Optimal generation mix with short-term demand response and wind penetration," *IEEE Trans. Power Syst.*, vol. 27, no. 2, pp. 830–839, May 2012.

[14] C. Sahin, M. Shahidehpour, and I. Erkmen, "Allocation of hourly reserve versus demand response for security-constrained scheduling of stochastic wind energy," *IEEE Trans. Sustain. Energy*, vol. 4, no. 1, pp. 219–228, Jan. 2013.

[15] N. I. Nwulu and X. Xia, "Multi-objective dynamic economic emission dispatch of electric power generation integrated with game theory based demand response programs," *Energy Convers. Manage.*, vol. 89, pp. 963–974, Jan. 2015.

[16] E. Galvan, G. G. Alcaraz, and N. G. Cabrera, "Two-phase short-term scheduling approach with intermittent renewable energy resources and demand response," *IEEE Latin America Trans.*, vol. 13, no. 1, pp. 181–187, Jan. 2015.

[17] A. Zakariazadeh, S. Jadid, and P. Siano, "Stochastic operational scheduling of smart distribution system considering wind generation and demand response programs," *Int. J. Elect. Power Energy Syst.*, vol. 63, pp. 218–225, Dec. 2014.

[18] Y. Wang, Q. Xia, and C. Kang, "Unit commitment with volatile node injections by using interval optimization," *IEEE Trans. Power Syst.*, vol. 26, no. 3, pp. 1705–1713, Aug. 2011.

[19] L. Wu, M. Shahidehpour, and Z. Li, "Comparison of scenario-based and interval optimization approaches to stochastic SCUC," *IEEE Trans. Power Syst.*, vol. 27, no. 2, pp. 913–921, May 2012.

[20] D. Bienstock, M. Chertkov, and S. Harnett, "Chance-constrained optimal power flow: Risk-aware network control under uncertainty," *SIAM Rev.*, vol. 56, no. 3, pp. 461–495, Aug. 2014.

[21] A. Ben-Tal and A. Nemirovski, "Robust optimization—Methodology and applications," *Math. Program.*, vol. 92, no. 3, pp. 453–480, May 2002.

[22] M. Black and G. Strbac, "Value of bulk energy storage for managing wind power fluctuations," *IEEE Trans. Energy Convers.*, vol. 22, no. 1, pp. 197–205, Mar. 2007.

[23] *Comparison of Standards and Technical Requirements of Grid-Connected Wind Power Plants in China and the United States*, Standards GB/T 19963, 2011.

[24] D. C. Kiplangat, K. Asokan, and K. S. Kumar, "Improved week-ahead predictions of wind speed using simple linear models with wavelet decomposition," *Renew. Energy*, vol. 93, pp. 38–44, Aug. 2016.

[25] H. A. Aalami, M. P. Moghaddam, and G. R. Yousefi, "Demand response modeling considering interruptible/curtailable loads and capacity market programs," *Appl. Energy*, vol. 87, no. 1, pp. 243–250, Jan. 2010.

[26] Z. Li, R. Ding, and C. A. Floudas, "A comparative theoretical and computational study on robust counterpart optimization: I. Robust linear optimization and robust mixed integer linear optimization," *Ind. Eng. Chem. Res.*, vol. 50, no. 18, pp. 10567–10603, Jul. 2011.

[27] K. Zhang *et al.*, "Optimal design of hybrid energy storage system capacity for wind farms," *CSEE*, vol. 32, no. 25, pp. 79–87, Sep. 2012.

[28] M. M. Etghani, M. H. Shojaeefard, A. Khalkhali, and M. Akbari, "A hybrid method of modified NSGA-II and TOPSIS to optimize performance and emissions of a diesel engine using biodiesel," *Appl. Thermal Eng.*, vol. 59, nos. 1–2, pp. 309–315, Sep. 2013.

WENFEI YI (S'16) received the M.S. degree from North China Electric Power University, Beijing, China, in 2014, where he is currently pursuing the Ph.D. degree. His research interests include the planning of demand response and the scheduling of integrated energy systems.

YIWEI ZHANG (S'17) received the B.S. degree from North China Electric Power University, Beijing, China, in 2017, where he is currently pursuing the M.S. degree. His research interest includes the operation of IES.

ZHIBIN ZHAO (M'17) received the Ph.D. degree in electrical engineering from North China Electric Power University, Beijing, China, in 2005. He is currently a Professor with the State Key Laboratory of Alternate Electrical Power System with Renewable Energy Sources, North China Electric Power University. His current research interests include renewable energy power systems, computational electromagnetics, and electromagnetic compatibility in high-power electronic devices.

YONGZHANG HUANG (M'14) received the Ph.D. degree in physics from the Chinese Academy of Sciences in 1991. He is currently a Professor with the Department of Electrical Engineering, North China Electric Power University, Beijing. His current research interests include renewable energy power systems, high-power electronic devices and applications, electric vehicles, and big data of the power grid.